Sensors & Actuators B, Chemical,

Devoted to the Late Dr. Tetsuro Seiyama

Title:

Solid Electrolyte NOx Sensor Using Pyrochlore -Type Oxide Electrode

Return to:

Dr. Youichi SHIMIZU

Department of Applied Chemistry, Faculty of Engineering,

Kyushu Institute of Technology,

1-1 Sensui-cho, Tobata, Kitakyushu 804-0015, Japan

Solid Electrolyte NOx Sensor Using Pyrochlore -Type Oxide Electrode

Youichi Shimizu* and Koji Maeda

Department of Applied Chemistry, Kyushu Institute of Technology,

1-1 Sensui-cho, Tobata, Kitakyushu 804-0015, Japan

Abstract

Solid electrolyte electrochemical devices based on sodium super-ionic conductor (NASICON: $Na_{1+x}Zr_2Si_xP_{3-x}O_{12}$) and pyrochlore-type oxide ($Pb_2M_2O_{7-y}$: M= Ir, $Ru_{1-x}Pb_x$; x=0 - 0.75) electrodes were found to exhibit good performance for the potentiometric sensing of NO as well as NO_2 at 400°C. The EMF responses were almost linear to the logarithm of NO or NO_2 concentration. Among the elements tested, the device attached with $Pb_2Ru_{1.5}Pb_{0.5}O_{7-y}$ electrode gave excellent NO sensing properties, and the EMF changed with changing gas concentration of NO diluted in N_2 or NO diluted in an O_2 and N_2 mixture with negative or positive slope, respectively, while it kept almost constant to the concentration change of NO_2 and CO_2 diluted in air.

Keywords: Pyrochlore-type oxide, NOx sensor, NASICON, Solid electrolyte

---

*Corresponding author. Fax: +81 93 884 3323, e-mail: shims@che.kyutech.ac.jp

1. Introduction

Monitoring of nitrogen oxides (NOx: NO and NO_2) as serious gas pollutants is becoming very important for the protection of global environments. Among compact NOx sensors, the electrochemical cell type based on solid electrolytes [1-5] is of particular interest from the view points of sensitivity, selectivity, and simple element structure. Most of the solid electrolyte NOx sensors so far investigated have generally used nitrate-based metal salts as an auxiliary phase, and they are not intrinsically suited for detection of NO, which is the major component of NOx in combustion exhausts. Recently, solid electrolyte sensor elements using sodium nitrite [6, 7] or nitrate-based binary systems [8] were reported to show high sensitivity to NO as well as NO_2. However they still have problems for chemical and/or thermal stability of the materials. Solid-state electrochemical elements, which combine solid electrolytes with oxide-based electrode, seem to bring about high chemical and thermal stability, and the devices for CO [9], CO_2 [10], and H_2S [11] have been proposed. It was also reported that the use of metal oxide electrodes, such as $CdMn_2O_4$ [12] and Cr_2O_3 [13], instead of conventional metal salts for the auxiliary phase of solid electrolyte NOx sensor seems to bring about better sensing performance to NO and/or NO_2 as well as stability at higher temperatures. It has been reported that the oxide electrode used at an auxiliary phase acts as an electrode catalyst and the response is based on the change of mixed potential at the electrode reactions. In our previous study [13], it was seen that some NOx sensor elements attached with metal oxide thin-film electrodes have high sensitivities to NO and/or NO_2, however most of which lack stability in the atmosphere including NOx gases. It is well known that pyrochlore-type oxides such as Pb-Ru-O and Pb-Ir-O systems have high chemical stability even in an acidic solution as well as high catalytic activities to oxygen reduction and/or oxygen evolution [14-16]. In this study, we have tried to use pyrochlore-type oxide electrodes for solid electrolyte-based NO and/or NO_2

sensors. It has turned out that the devices using pyrochlore-type oxide have high sensitivities and stability to NO as well as NO_2 at 400 °C. It was further found that the device attached with $Pb_2[Ru_{1.5}Pb_{0.5}]O_{7-y}$ showed higher sensitivity to NO than that to NO_2 at 400°C.

2. Experimental

2.1 Pyrochlore-type oxide preparation

Pyrochlore-type oxides ($Pb_2Ru_{2-x}Pb_xO_{7-y}$: x= 0 - 0.75, $Pb_2Ir_2O_{7-y}$) were prepared by a precipitation method [15, 16]. An aqueous solution was obtained by dissolving starting materials, Ru- and Ir- chlorides and Pb nitride of special grade reagents (Kishida Chemical Co., Ltd.), in a proportion of desired pyrochlore-type oxides. Then, an excess amount of 2 mol·dm^{-3} NaOH was added slowly to the solution and co-precipitation was carried out at 75°C under constant stirring and purging with oxygen for 24h. The filtered products were dried at 120°C for 12h and calcined at 500 - 780 °C for 2h in atmospheric air. The obtained materials were washed with distilled water for removing a by-product, NaCl, and then finally dried at 120°C for 12h. The products were characterized with X-ray diffraction analysis (XRD) (JDX-3500K, JEOL Ltd.) using Cu-Kα radiation. Figure 1 shows XRD patterns of $Pb_2Ir_2O_{7-y}$ and $Pb_2Ru_2O_{7-y}$ powders after calcined at 780 and 500 °C, respectively. Although a slight impurity phase of RuO_2 was seen only for the $Pb_2Ru_2O_{7-y}$, most of the powders obtained with this method showed well crystallized and almost single-phase oxides.

2.2 Sensor measurements

Figure 2 shows a schematic diagram of NOx sensor element using pyrochlore-type oxide electrodes. A NASICON ($Na_3Zr_2Si_2PO_{12}$) disc, 11 mm in diameter and 0.8 mm thick, prepared by a sol-gel method using aqueous solution [17, 18], was fixed on an alumina tube with a ceramic adhesive. Oxide

electrodes were fabricated by a painting method [19], i.e., powders of the prepared pyrochlore-type oxides or RuO_2 (Mitsuwa Chemical Co. Ltd.) were kneaded with a small portion of turpentine oil (Kishida Chemical Co. Ltd.), and a paste thus obtained was painted onto the surface of the NASICON disc, and dried and finally sintered at 500 ℃ for 1 h to form a layer of oxide as a sensing electrode. An Au mesh was attached on the top of the oxide layer to connect a Pt-wire lead. A reference Pt electrode attached on the inside surface of the NASICON disc was always exposed to static atmospheric air. NOx sensing experiments were carried out in a conventional flow apparatus equipped with a heating facility at 100-500 ℃. Sample gases containing NO or NO_2 were prepared from each parent gas, i.e., NO diluted with nitrogen or NO_2 diluted with a dry synthetic air (N_2+O_2 gas mixture), by mixing it with N_2 (99.999 vol%) or the air. The sensor response, EMF, was measured with a digital electrometer (R8240; Advantest Corp.) at a total flow rate of 100 cm^3/min.

3. Results and Discussion

3.1 $Pb_2M_2O_{7-y}$ (M= Ir, Ru) electrodes

First, NO_2 sensing performance of NASICON-based sensor elements combined with $Pb_2Ir_2O_{7-y}$ or $Pb_2Ru_2O_{7-y}$ was investigated. As shown in Fig. 3, both devices responded rather well to NO_2. The EMF responses were linear to the logarithm of NO_2 concentration ($\log P_{NO2}$) between 20 and 200 ppm with both positive slopes of +50 mV/decade or +30 mV/decade for the elements using $Pb_2Ir_2O_{7-y}$ or $Pb_2Ru_2O_{7-y}$, respectively. The $Pb_2Ir_2O_{7-y}$ based element showed rather quick response to NO_2, i.e., the 90% response time for the concentration change from 110 ppm to 220 ppm NO_2 in air was as short as 30s at 400°C. $Pb_2Ru_2O_{7-y}$ based element, on the other hand, showed a unique transient curve and the EMF value at each concentration gave a steady value within about 5-20 min.

It was further found that these devices could also respond to NO diluted in N_2 at the examined concentration range between 50 and 1000 ppm at 400 °C, with the 90% response time of about 1-10 min., as shown in Fig. 4. Both EMF changes (ΔE) were linear to the logarithm of NO concentration ($\log P_{NO}$), with negative slopes of -29 mV/decade or -86 mV/decade for the elements using $Pb_2Ir_2O_{7-y}$ or $Pb_2Ru_2O_{7-y}$, respectively.

Dependence of the sensing performance to NOx on operation temperatures was further investigated by using the $Pb_2Ir_2O_{7-y}$ based element. For NO_2 sensing, the element showed EMF responses at the examined temperatures between 100 and 400°C. EMF responses increased with increasing NO_2 concentration at each temperature, being linear to $\log P_{NO2}$, with all positive slopes. The magnitude of the slopes decreased with increasing operation temperature, as shown in Fig. 5 (a). At temperatures below 300°C, it was hard to recover the initial EMF value when switching back to air. For NO sensing, the element also showed EMF responses at the examined temperatures between 200 and 500°C. The EMF values decreased with increasing NO concentration, and showed linear relationship between EMF and $\log P_{NO}$ with all negative slopes at the all temperatures examined. As shown in Fig. 5 (b), the slope for EMF vs. $\log P_{NO}$, the sensitivity to NO, decreased with increasing operation temperature. On the other hand, the reversibility of the responses became poor with decreasing operation temperature. The quickest response rate and the complete reversibility of EMF response were obtained at the operation temperature of 400°C for NO as well as NO_2. It still has high sensitivities of -29 mV/decade and +50 mV/decade for NO and NO_2, respectively at 400°C. Thus, the best operation temperature should be 400°C for NO_2 as well as NO sensing.

The reason for the dependence of the sensor responses on operation temperature was not clear yet, but it seems to come from the catalytic activity and/or sorption-desorption properties of the pyrochlore-type oxide electrodes to the

reaction gases. Further investigation is now in progress. Hereafter, operation temperature has been fixed at 400°C.

3.2 $Pb_2[Ru_{2-x}Pb_x]O_{7-y}$ electrodes

As $Pb_2Ru_2O_{7-y}$ based element showed higher sensitivity to NO than that to NO_2, i.e., the slope for NO was three times as high as that for NO_2, the Pb-Ru-O family has been further studied as the electrode materials.

NOx sensing performance of the various sensor elements based on $Pb_2[Ru_{2-x}Pb_x]O_{7-y}$ as well as $Pb_2Ir_2O_{7-y}$ electrodes at 400°C was summarized in Fig. 6 (a, b). All devices based on the Pb-(Ru/Pb)-O system showed higher EMF responses to the sample gases containing NO than that on $Pb_2Ir_2O_{7-y}$. It was further found that the sensor elements using the Pb-(Ru/Pb)-O system except $Pb_2Ru_{1.25}Pb_{0.75}O_{7-y}$ (x= 0.75) showed high sensitivity to NO than that to NO_2. NO sensitivity, the slope of EMF vs. $\log P_{NO}$, decreased with increasing x in $Pb_2[Ru_{2-x}Pb_x]O_{7-y}$, although it still has high sensitivity of -35mV/decade even at x= 0.75. Surprisingly, it was found that the $Pb_2Ru_{1.5}Pb_{0.5}O_{7-y}$ (x= 0.5) / NASICON combination showed only a little NO_2 sensitivity at the concentration range between 20 and 220 ppm at 400°C, although it had good NO sensitivity. Figure 7 shows response transients to NO or NO_2 for the device using $Pb_2Ru_{1.5}Pb_{0.5}O_{7-y}$. Although the transient in NO_2 showed overshoot at switching NO_2 concentration, the each EMF at the different NO_2 concentration became a steady value of about +10 mV from the initial EMF value in air within about 20min. The device showed poor NO_2 sensitivity, while it had good EMF response to NO diluted in N_2, with a 90% response time of about 2-10 min. Figure 8 shows dependence of EMF of the sensor device using the $Pb_2Ru_{1.5}Pb_{0.5}O_{7-y}$ / NASICON combination on gas concentration. The sensor hardly responded to NO_2 and CO_2 diluted in air, while it showed high EMF

response to NO diluted in N_2, being linear to $\log P_{NOx}$ with a negative slope of -40 mV/decade.

In order to discuss the sensing properties of the $Pb_2Ru_{2-x}Pb_xO_{7-y}$ system from the crystal structure, the lattice parameter of the pyrochlore-type oxides (cubic) was calculated. As shown in Fig. 9, the lattice parameter (a) of the $Pb_2Ru_{2-x}Pb_xO_{7-y}$ system increased with increasing x up to 0.50 and was saturated at around x=0.75. It was reported that $Pb_2Ru_2O_{7-y}$ is represented by the general formula, $Pb^{2+}{}_2[Ru^{4+}Ru^{5+}]O_{6.5}$ [15]. The present Pb-(Ru/Pb)-O system should be written as $Pb^{2+}{}_2[Ru^{4+}{}_{1-x'}Ru^{5+}{}_{1-x''}Pb^{4+}{}_x]O_{7-y}$ ($x = x' + x''$). The expansion of the unit cell is consistent with the difference in the ionic radii of Ru^{4+} (0.62A, and further small for Ru^{5+}) and Pb^{4+} (0.775A) [15]. $RuO_2(Ru^{4+})$-based element showed higher sensitivity to NO_2 than that to NO, as shown in Fig. 6 (c). $PbO(Pb^{2+})$-based element also showed higher NO_2 sensitivity than NO in our previous study. High NO sensitivity of Pb-Ru-O family seems to come from the effect of Ru^{5+} in the lattice. The decrease in NO_2 sensitivity with increasing x up to 0.50 should be related to Pb^{4+} and/or oxygen vacancy in the systems. Further studies should be necessary to clarify the electrode systems more quantitatively.

In order to examine the NOx sensing mechanism, the effect of co-existent oxygen on the measurement of NO concentration was tested for the $Pb_2Ru_{1.5}Pb_{0.5}O_{7-y}$ based device. As shown in Fig. 10, the element showed rather well EMF response to NO co-existed 10% oxygen with linear relationship between EMF vs. $\log P_{NO}$. However, the slope of +43 mV/decade was completely different in sign from that for NO in N_2 (Fig. 8 (a)).

As mentioned above, the sensor signal was largely influenced by the coexisted oxygen. The mixed potential mechanism [12] should proceed on the sensing electrode. Therefore, the each EMF value could be determined by the potential at which cathodic and anodic reactions proceed at an equal rate. For

NO_2 sensing, the following electrochemical reactions (1) and (2) are assumed for the cathodic and anodic reactions, respectively.

$$NO_2 + 2e^- = NO + O^{2-} \quad (1)$$

$$O^{2-} = (1/2)O_2 + 2e^- \quad (2)$$

For NO sensing, the reactions changed drastically by the coexisted oxygen. When the co-existed oxygen is rare (NO sensing in N_2), reactions (3) and (4) are assumed for the cathodic and anodic reactions, respectively. When an enough amount of oxygen is co-existed, reactions (5) and (2) are assumed for the cathodic and anodic reactions, respectively.

$$NO + O^{2-} = NO_2 + 2e^- \quad (3)$$

$$(1/2)O_2 + 2e^- = O^{2-} \quad (4)$$

$$NO + O_2 + 2e^- = NO_2 + O^{2-} \quad (5)$$

Oxygen in reaction (4) should be considered as an impurity (10ppm O_2) of N_2 gas used. However, the sensing mechanisms of the present electrochemical device still need further investigations.

4. Conclusion

Solid electrolyte NOx sensor using NASICON and pyrochlore-type oxide ($Pb_2M_2O_{7-y}$; M=Ir, $Ru_{1-x}Pb_x$: x = 0 - 0.75) electrodes were found to exhibit good performance for the potentiometric sensing of NO as well as NO_2 at 400°C. EMF responses were linear to the logarithm of NO or NO_2 concentration. The device attached with $Pb_2Ru_{1.5}Pb_{0.5}O_{7-y}$ electrode gave excellent NO sensing properties. The mixed potential should be considered for the sensing mechanism.

Acknowledgments

The authors are grateful to Mr. Hiroyuki Suzuki for his assistance for preparation of oxide samples and to the Center for Instrumental Analysis, Kyushu Institute of Technology for XRD measurement.

References

[1] M. Gauthier and A. Chamberland, Solid-state detectors for the potentiometric determination of gaseous oxides, I. Measurement in air, *J. Electrochem. Soc.*, **124** (1977) 1579-1583.

[2] G. Hötzel and W. Weppner, Application of fast ionic conductors in solid state galvanic cells for gas sensors, *Solid State Ionics*, **18/19** (1986) 1223-1227.

[3] G. Hötzel and W. Weppner, Potentiometric gas sensors based on fast solid electrolyte, *Sensors & Actuators B*, **12** (1987) 449-453.

[4] N. Rao, C.M. Bleek, and J. Schoonman, Potentiometric NOx (x=1,2) sensors with Ag^{+}-β"-alumina as solid electrolyte and Ag metal as solid reference, *Solid State Ionics*, **52** (1992) 339-346.

[5] Y. Shimizu, Y. Okamoto, S. Yao, N. Miura, and N. Yamazoe, Solid electrolyte NO_2 sensors fitted with sodium nitrate and/or barium nitrate electrodes, *Denki Kagaku*, **59** (1991) 465-472.

[6] S. Yao, Y. Shimizu, N. Miura, and N. Yamazoe, Use of sodium nitrite auxiliary electrode for solid electrolyte sensor to detect nitrogen oxides, *Chem. Lett.*, **1992** (1992) 587-590.

[7] N. Miura, S. Yao, Y. Shimizu, and N. Yamazoe, Development of high-performance solid-electrolyte sensors for NO and NO_2, *Sensors & Actuators B*, **13/14** (1993) 387-390.

[8] H. Kurosawa, Y. Yan, N. Miura, and N. Yamazoe, Stabilized zirconia-based potentiometric sensor for nitrogen oxides, *Chem. Lett.*, **1994** (1994) 1733-1736.

[9] H. Okamoto, H. Obayashi, and T. Kudo, Carbon monoxide gas sensor made of stabilized zirconia, *Solid State Ionics*, **1** (1980) 319-326.

[10] S. Brediklin, J. Liu, and W. Weppner, Solid ionic conductor/ semiconductor junctions for chemical sensors, *Appl. Phys. A*, **57** (1993) 37-43.

[11] Y. Yan, N. Miura, and N. Yamazoe, Potentiometric sensor using stabilized zirconia and tungsten oxide for hydrogen sulfide, *Chem. Lett.*, **1994** (1994) 1753-1756.

[12] N. Miura, G. Lu, N. Yamazoe, H. Kurosawa, and M. Hasei, Mixed potential type NOx sensor based on stabilized zirconia and oxide electrode, *J. Electrochem. Soc.*, **143** (1996) L33-L35.

[13] Y. Shimizu and K. Maeda, Solid electrolyte-based NOx sensor using auxiliary phase of metal oxide, *Chem. Lett.*, **1996** (1996) 117-118.

[14] J. M. Longo, P. M. Raccah, and J. B. Goodenough, $Pb_2M_2O_{7-x}$ (M=Ru, Ir, Re) - preparation and properties of oxygen deficient pyrochlores, *Mat. Res. Bull.*, **4** (1969) 191-202.

[15] H. S. Horowitz, J. M. Longo, J. T. Lewandowski, New oxide pyrochlores: $A_2[B_{2-x}A_x]O_{7-y}$ (A= Pb, Bi; B= Ru, Ir), *Mat. Res. Bull.*, **16** (1981) 489-496.

[16] J. M. Zen, R. Manoharan, J. B. Goodenough, Oxygen reduction on Ru-oxide pyrochlores bonded to a proton-exchange membrane, *J. Appl. Electrochem.*, **22** (1992) 140-150.

[17] Y. Shimizu, S. Michishita, and T. Murata, Preparation of sodium ionic conductor based on sol-gel method using aqueous solution, *Jpn. J. Appl. Phys.*, **34** (1995) L833-L836.

[18] Y. Shimizu, Y. Azuma, and S. Michishita, Sol-gel synthesis of NASICON discs from aqueous solution, *J. Mater. Chem.*, **7** (1997) 1487-1490.

[19] T. Inoue, N. Seki, K. Eguchi, and H. Arai, Low-temperature operation of solid electrolyte oxygen sensors using perovskite-type oxide electrodes and cathodic reaction kinetics, *J. Electrochem. Soc.*, **137** (1990) 2523-2527.

Biographies

Youichi Shimizu has been an associate professor at Kyushu Institute of Technology since 1993. He received the B. Eng. degree in applied chemistry in 1983 and the Dr. Eng. degree in 1992 from Kyushu University. His current research interests include the solid-state gas sensors and ion sensors.

Koji Maeda received his B. Eng. degree in applied chemistry in 1995 and the M. Eng. degree in 1997 from Kyushu Institute of Technology. He is currently working at Takagi Co., Ltd.

Figure captions

Fig. 1 XRD patterns of $Pb_2Ir_2O_{7-y}$ (a) or $Pb_2Ru_2O_{7-y}$ (b) powders after calcined at 780°C or 500°C, respectively.

Fig. 2 Schematic diagram of NOx sensor device using NASICON and pyrochlore- type oxide electrode.

Fig. 3 Sensing performance to NO_2 of the devices using $Pb_2Ir_2O_{7-y}$ (a) or $Pb_2Ru_2O_{7-y}$ (b) electrodes at 400°C.

Fig. 4 Sensing performance to NO of the devices using $Pb_2Ir_2O_{7-y}$ (a) or $Pb_2Ru_2O_{7-y}$ (b) at 400°C.

Fig. 5 Effect of operation temperature on the sensing properties to NO_2 (a) or NO (b) of $Pb_2Ir_2O_{7-y}$ based element.

Fig. 6 Sensing performance to NO_2 or NO of the various sensor devices using $Pb_2Ru_{2-x}Pb_xO_{7-y}$ (x=0~0.75) (a), $Pb_2Ir_2O_{7-y}$ (b), and RuO_2 (c) electrodes at 400°C.

Fig. 7 Response transients to NO_2 (a) or NO (b) of the device using $Pb_2Ru_{1.5}Pb_{0.5}O_{7-y}$ at 400°C.

Fig. 8 Sensing performance of the device using $Pb_2Ru_{1.5}Pb_{0.5}O_{7-y}$ electrode to NO in N_2 (a), NO_2 in air (b), and CO_2 in air (c) at 400°C.

Fig. 9 Effect of partial substitution of Pb for Ru site on the lattice parameter (a) for $Pb_2Ru_{2-x}Pb_xO_{7-y}$ (x=0~0.75) system.

Fig. 10 NO sensing performance of the device using $Pb_2Ru_{1.5}Pb_{0.5}O_{7-y}$ electrode under coexisted oxygen (10%) at 400°C.

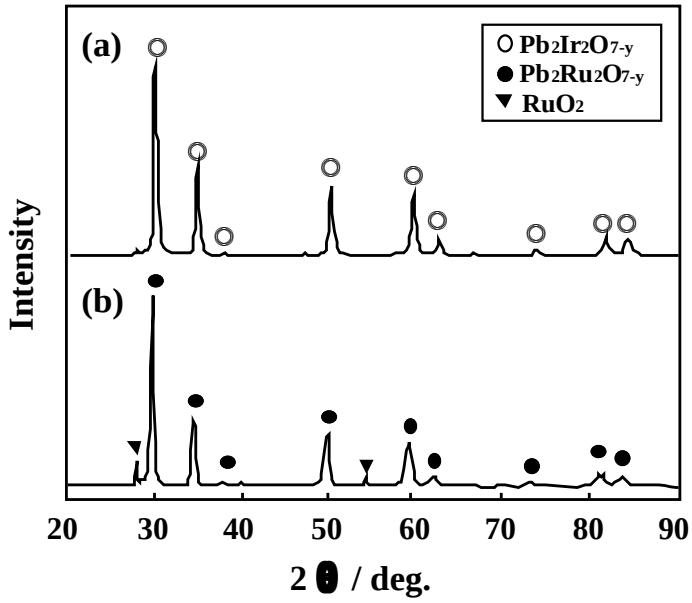

Fig. 1 XRD patterns of $Pb_2Ir_2O_{7-y}$ (a) or $Pb_2Ru_2O_{7-y}$ (b) powders after calcined at 780°C or 500°C, respectively.

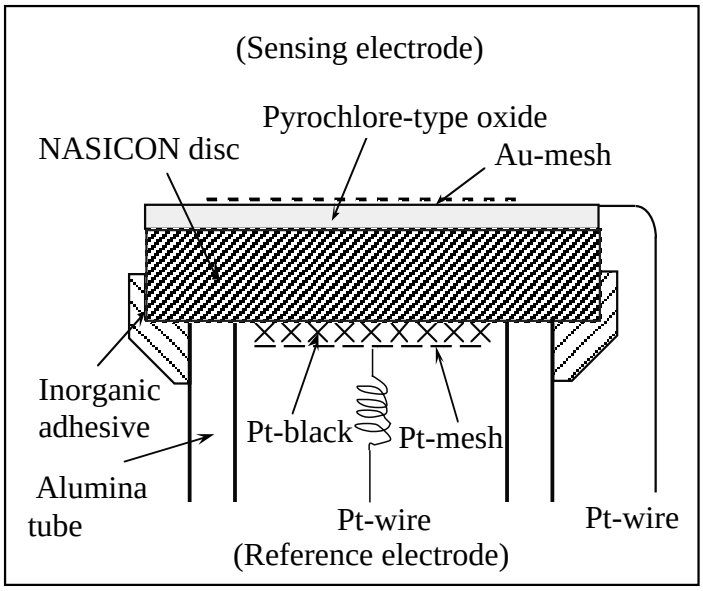

Fig. 2 Schematic diagram of NOx sensor device using NASICON and pyrochlore-type oxide electrode.

Y. Shimizu et al.

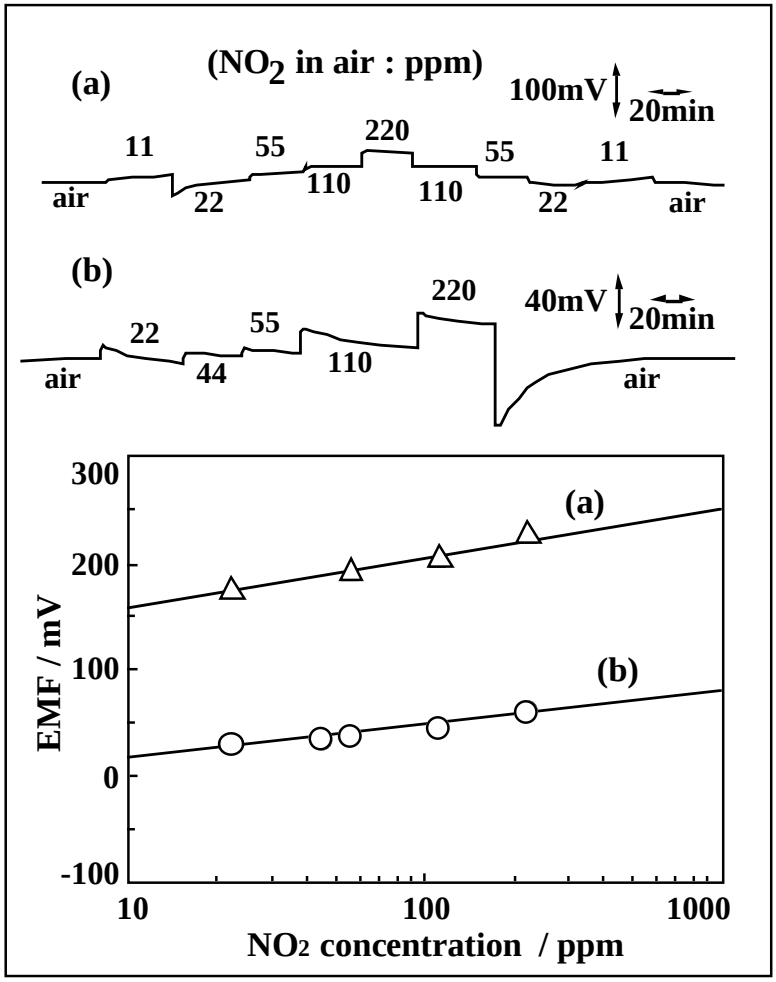

Fig. 3 Sensing performance to NO_2 of the devices using $Pb_2Ir_2O_{7-y}$ (a) or $Pb_2Ru_2O_{7-y}$ (b) electrodes at 400°C.

Y. Shimizu et al.

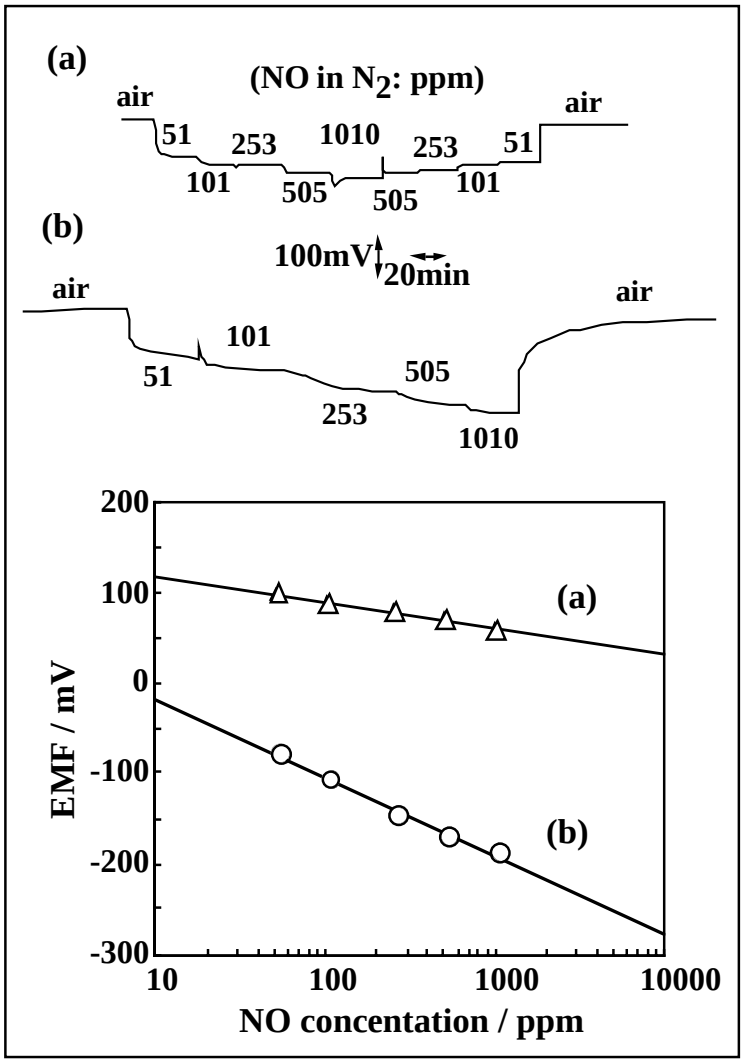

Fig. 4 Sensing performance to NO of the devices using $Pb_2Ir_2O_{7-y}$ (a) or $Pb_2Ru_2O_{7-y}$ (b) at 400°C.

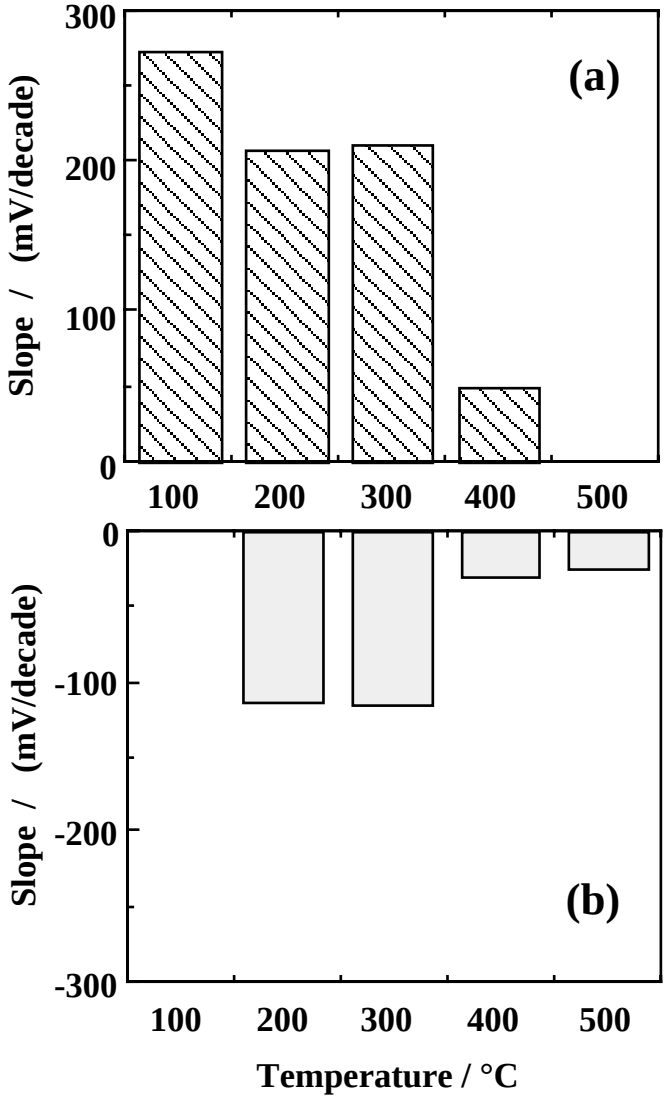

Fig. 5 Effect of operation temperature on the sensing properties to NO_2 (a) or NO (b) of $Pb_2Ir_2O_{7-y}$ based element.

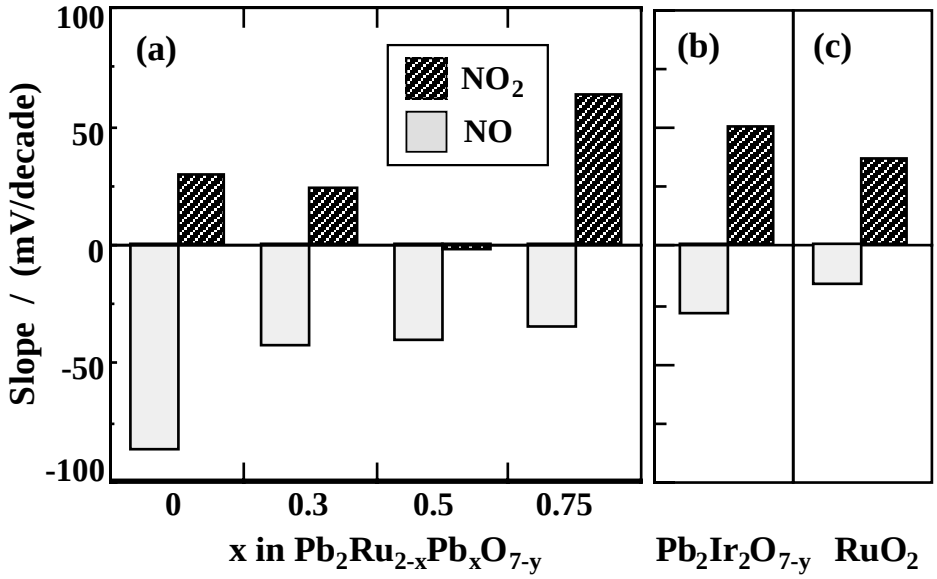

Fig. 6 Sensing performance to NO_2 or NO of the various sensor devices using $Pb_2Ru_{2-x}Pb_xO_{7-y}$ (x=0~0.75) (a), $Pb_2Ir_2O_{7-y}$ (b), and RuO_2 (c) electrodes at 400°C.

Y. Shimizu et al.

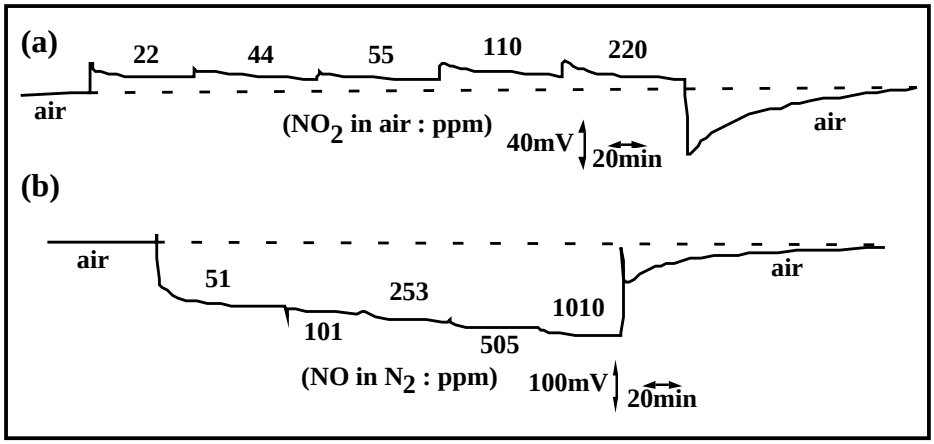

Fig. 7 Response transients to NO_2 (a) or NO (b) of the device using $Pb_2Ru_{1.5}Pb_{0.5}O_{7-y}$ at 400°C.

Y. Shimizu et al.

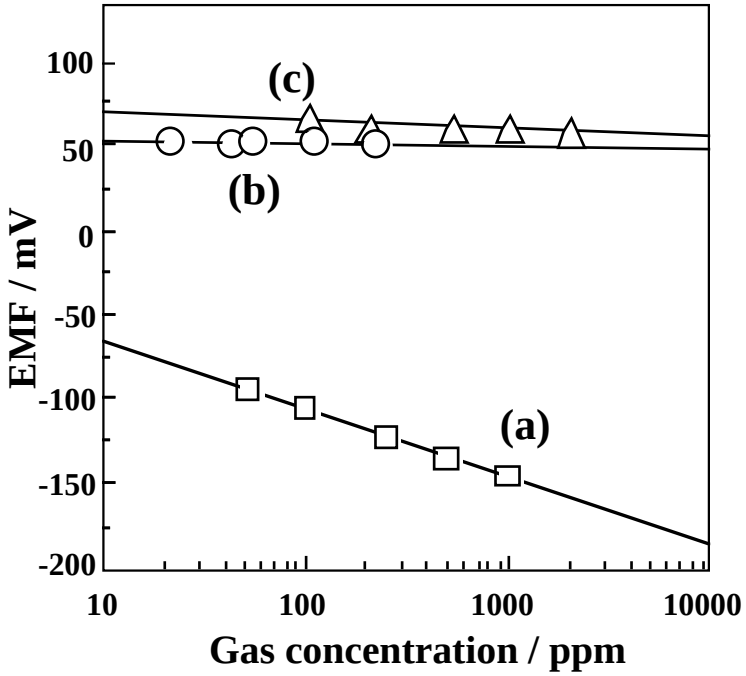

Fig. 8 Sensing performance of the device using $Pb_2Ru_{1.5}Pb_{0.5}O_{7-y}$ electrode to NO in N_2 (a), NO_2 in air (b), and CO_2 in air (c) at 400°C.

Y. Shimizu et al.

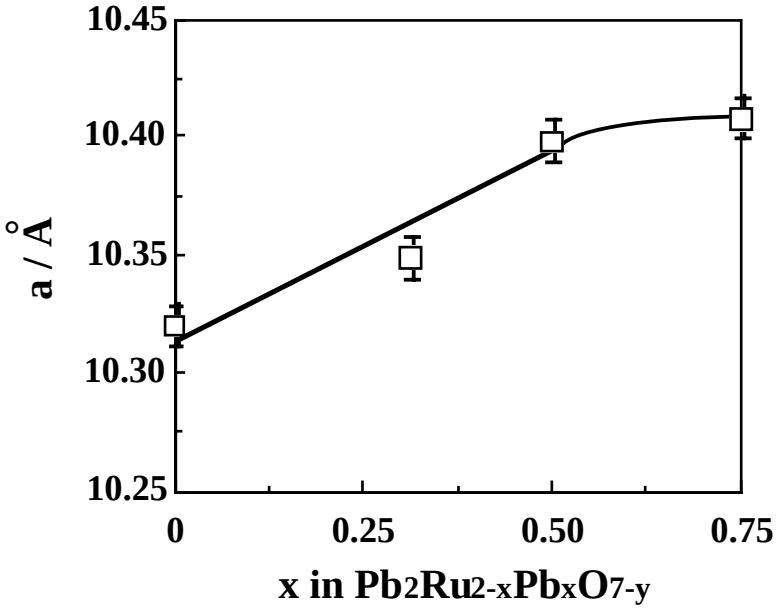

Fig. 9 Effect of partial substitution of Pb for Ru site on the lattice parameter (a) for $Pb_2Ru_{2-x}Pb_xO_{7-y}$ (x=0~0.75) system.

Y. Shimizu et al.

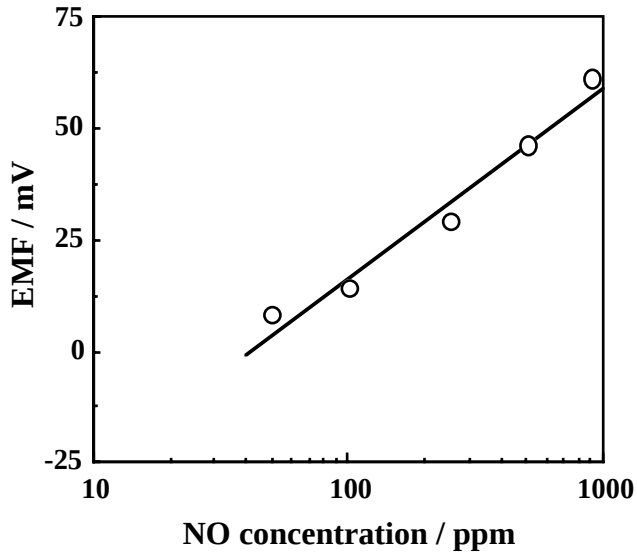

Fig. 10 NO sensing performance of the device using $Pb_2Ru_{1.5}Pb_{0.5}O_{7-y}$ electrode under coexisted oxygen (10%) at 400°C.

Y. Shimizu et al.